2

Fundamentals of Piezoelectricity

2.1 Introduction

This chapter is concerned with piezoelectric materials and their properties. We begin the chapter with a brief overview of some historical milestones, such as the discovery of the piezoelectric effect, the invention of piezoelectric ceramic materials, and commercial and military utilization of the technology. We will review important properties of piezoelectric ceramic materials and will then proceed to a detailed introduction of the piezoelectric constitutive equations.

The main assumption made in this chapter is that transducers made from piezoelectric materials are linear devices whose properties are governed by a set of tensor equations. This is consistent with the IEEE standards of piezoelectricity [154]. We will explain the physical meaning of parameters which describe the piezoelectric property, and will clarify how these parameters can be obtained from a set of simple experiments.

In this book, piezoelectric transducers are used as sensors and actuators in vibration control systems. For this purpose, transducers are bonded to a flexible structure and utilized as either a sensors to monitor structural vibrations, or as actuators to add damping to the structure. To develop model-based controllers capable of adding sufficient damping to a structure using piezoelectric actuators and sensors it is vital to have models that describe the dynamics of such systems with sufficient precision.

We will explain how the dynamics of a flexible structure with incorporated piezoelectric sensors and actuators can be derived starting from physical principles. In particular, we will emphasize the structure of the models that are obtained from such an exercise. Knowledge of the model structure is crucial to the development of precise models based on measured frequency domain data. This will constitute our main approach to obtaining models of systems studied throughout this book.

2.2 History of Piezoelectricity

The first scientific publication describing the phenomenon, later termed as piezoelectricity, appeared in 1880 [48]. It was co-authored by Pierre and Jacques Curie, who were conducting a variety of experiments on a range of crystals at the time. In those experiments, they cataloged a number of crystals, such as tourmaline, quartz, topaz, cane sugar and Rochelle salt that displayed surface charges when they were mechanically stressed.

In the scientific community of the time, this observation was considered as a significant discovery, and the term "piezoelectricity" was coined to express this effect. The word "piezo" is a Greek word which means "to press". Therefore, piezoelectricity means electricity generated from pressure - a very logical name. This terminology helped distinguish piezoelectricity from the other related phenomena of interest at the time; namely, contact electricity[1] and pyroelectricity[2].

The discovery of the direct piezoelectric effect is, therefore, credited to the Curie brothers. They did not, however, discover the converse piezoelectric effect. Rather, it was mathematically predicted from fundamental laws of thermodynamics by Lippmann [118] in 1881. Having said this, the Curies are recognized for experimental confirmation of the converse effect following Lippmann's work.

The discovery of piezoelectricity generated significant interest within the European scientific community. Subsequently, roughly within 30 years of its discovery, and prior to World War I, the study of piezoelectricity was viewed as a credible scientific activity. Issues such as reversible exchange of electrical and mechanical energy, asymmetric nature of piezoelectric crystals, and the use of thermodynamics in describing various aspects of piezoelectricity were studied in this period.

The first serious application for piezoelectric materials appeared during World War I. This work is credited to Paul Langevin and his co-workers in France, who built an ultrasonic submarine detector. The transducer they built was made of a mosaic of thin quartz crystals that was glued between two steel plates in a way that the composite system had a resonance frequency of 50 KHz. The device was used to transmit a high-frequency chirp signal into the water and to measure the depth by timing the return echo. Their invention, however, was not perfected until the end of the war.

Following their successful use in sonar transducers, and between the two World Wars, piezoelectric crystals were employed in many applications. Quartz crystals were used in the development of frequency stabilizers for vacuum-tube oscillators. Ultrasonic transducers manufactured from piezoelectric crystals were used for measurement of material properties. Many of the classic piezoelectric applications that we are familiar with, applications such

[1] Static electricity generated by friction
[2] Electricity generated from crystals, when heated

as microphones, accelerometers, ultrasonic transducers, etc., were developed and commercialized in this period.

Development of piezoceramic materials during and after World War II helped revolutionize this field. During World War II, significant research was performed in the United States and other countries such as Japan and the former Soviet Union which was aimed at the development of materials with very high dielectric constants for the construction of capacitors. Piezoceramic materials were discovered as a result of these activities, and a number of methods for their high-volume manufacturing were devised. The ability to build new piezoelectric devices by tailoring a material to a specific application resulted in a number of developments, and inventions such as: powerful sonars, piezo ignition systems, sensitive hydrophones and ceramic phono cartridges, to name a few.

2.3 Piezoelectric Ceramics

A piezoelectric ceramic is a mass of perovskite crystals. Each crystal is composed of a small, tetravalent metal ion placed inside a lattice of larger divalent metal ions and O_2, as shown in Figure 2.1.

To prepare a piezoelectric ceramic, fine powders of the component metal oxides are mixed in specific proportions. This mixture is then heated to form a uniform powder. The powder is then mixed with an organic binder and is formed into specific shapes, *e.g.* discs, rods, plates, etc. These elements are then heated for a specific time, and under a predetermined temperature. As a result of this process the powder particles sinter and the material forms a dense crystalline structure. The elements are then cooled and, if needed, trimmed into specific shapes. Finally, electrodes are applied to the appropriate surfaces of the structure.

Above a critical temperature, known as the "Curie temperature", each perovskite crystal in the heated ceramic element exhibits a simple cubic symmetry with no dipole moment, as demonstrated in Figure 2.1. However, at temperatures below the Curie temperature each crystal has tetragonal symmetry and, associated with that, a dipole moment. Adjoining dipoles form regions of local alignment called "domains". This alignment gives a net dipole moment to the domain, and thus a net polarization. As demonstrated in Figure 2.2 (a), the direction of polarization among neighboring domains is random. Subsequently, the ceramic element has no overall polarization.

The domains in a ceramic element are aligned by exposing the element to a strong, DC electric field, usually at a temperature *slightly below* the Curie temperature (Figure 2.2 (b)). This is referred to as the "poling process". After the poling treatment, domains most nearly aligned with the electric field expand at the expense of domains that are not aligned with the field, and the element expands in the direction of the field. When the electric field is removed most of the dipoles are locked into a configuration of near alignment

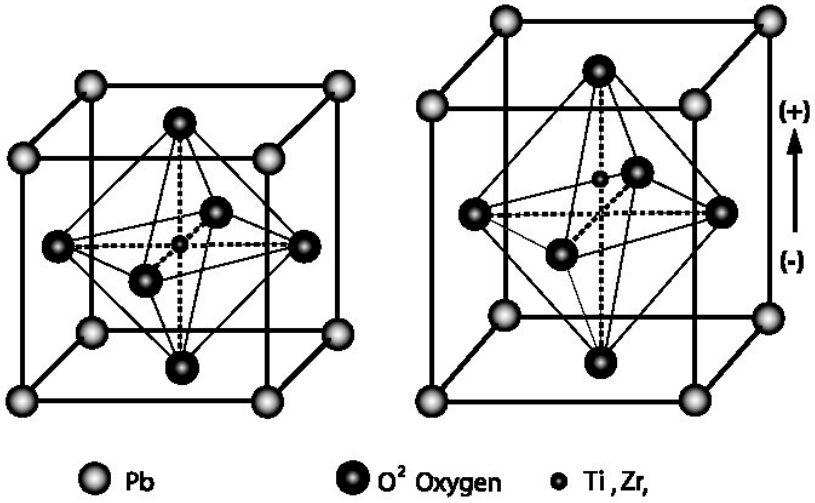

Figure 2.1. Crystalline structure of a piezoelectric ceramic, before and after polarization

(Figure 2.2 (c)). The element now has a permanent polarization, the remnant polarization, and is permanently elongated. The increase in the length of the element, however, is very small, usually within the micrometer range.

Properties of a poled piezoelectric ceramic element can be explained by the series of images in Figure 2.3. Mechanical compression or tension on the element changes the dipole moment associated with that element. This creates a voltage. Compression along the direction of polarization, or tension perpendicular to the direction of polarization, generates voltage of the same polarity as the poling voltage (Figure 2.3 (b)). Tension along the direction of polarization, or compression perpendicular to that direction, generates a voltage with polarity opposite to that of the poling voltage (Figure 2.3 (c)). When operating in this mode, the device is being used as a sensor. That is, the ceramic element converts the mechanical energy of compression or tension into electrical energy. Values for compressive stress and the voltage (or field

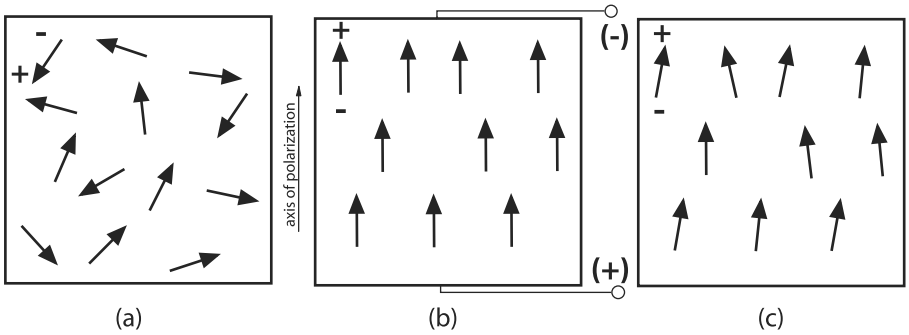

Figure 2.2. Poling process: (a) Prior to polarization polar domains are oriented randomly; (b) A very large DC electric field is used for polarization; (c) After the DC field is removed, the remnant polarization remains.

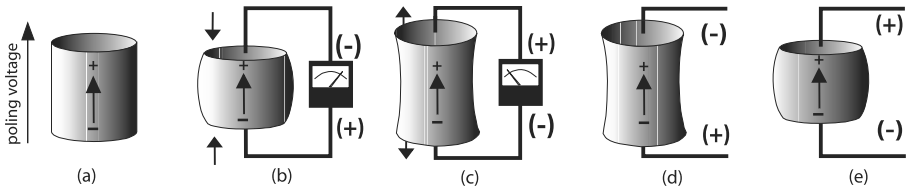

Figure 2.3. Reaction of a poled piezoelectric element to applied stimuli

strength) generated by applying stress to a piezoelectric ceramic element are linearly proportional, up to a specific stress, which depends on the material properties. The same is true for applied voltage and generated strain[3].

If a voltage of the same polarity as the poling voltage is applied to a ceramic element, in the direction of the poling voltage, the element will lengthen and its diameter will become smaller (Figure 2.3 (d)). If a voltage of polarity opposite to that of the poling voltage is applied, the element will become shorter and broader (Figure 2.3 (e)). If an alternating voltage is applied to the device, the element will expand and contract cyclically, at the frequency of the applied voltage. When operated in this mode, the piezoelectric ceramic is used as an actuator. That is, electrical energy is converted into mechanical energy.

2.4 Piezoelectric Constitutive Equations

In this section we introduce the equations which describe electromechanical properties of piezoelectric materials. The presentation is based on the IEEE standard for piezoelectricity [154] which is widely accepted as being a good representation of piezoelectric material properties. The IEEE standard assumes that piezoelectric materials are linear. It turns out that at low electric fields and at low mechanical stress levels piezoelectric materials have a linear profile. However, they may show considerable nonlinearity if operated under a high electric field or high mechanical stress level. In this book we are mainly concerned with the linear behavior of piezoelectric materials. That is, for the most part, we assume that the piezoelectric transducers are being operated at low electric field levels and under low mechanical stress.

When a poled piezoelectric ceramic is mechanically strained it becomes electrically polarized, producing an electric charge on the surface of the material. This property is referred to as the "direct piezoelectric effect" and is the

[3] It should be stressed that this statement is true when the piezoelectric material is being operated under small electric field, or mechanical stress. When subject to higher mechanical, or electrical fields, piezoelectric transducers display hysteresis-type nonlinearity. For the most part, in this monograph, the linear behavior of piezoelectric transducers will be of interest. However, Chapter 11 will briefly review the issues arising when a piezoelectric transducer is operated in the nonlinear regime.

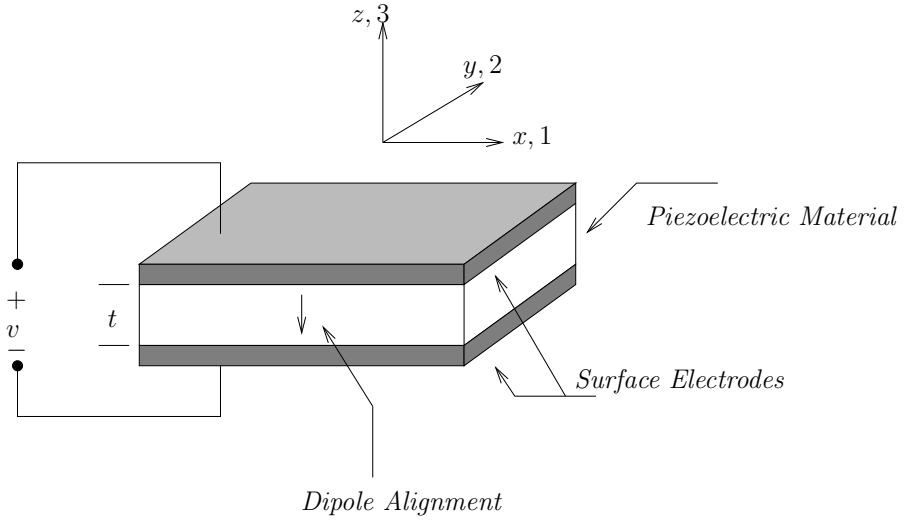

Figure 2.4. Schematic diagram of a piezoelectric transducer

basis upon which the piezoelectric materials are used as sensors. Furthermore, if electrodes are attached to the surfaces of the material, the generated electric charge can be collected and used. This property is particularly utilized in piezoelectric shunt damping applications to be discussed in Chapter 4.

The constitutive equations describing the piezoelectric property are based on the assumption that the total strain in the transducer is the sum of mechanical strain induced by the mechanical stress and the controllable actuation strain caused by the applied electric voltage. The axes are identified by numerals rather than letters. In Figure 2.4, 1 refers to the x axis, 2 corresponds to the y axis, and 3 corresponds to the z axis. Axis 3 is assigned to the direction of the initial polarization of the piezoceramic, and axes 1 and 2 lie in the plane perpendicular to axis 3. This is demonstrated more clearly in Figure 2.5.

The describing electromechanical equations for a linear piezoelectric material can be written as [154, 70]:

$$\varepsilon_i = S_{ij}^E \sigma_j + d_{mi} E_m \tag{2.1}$$

$$D_m = d_{mi} \sigma_i + \xi_{ik}^\sigma E_k, \tag{2.2}$$

where the indexes $i, j = 1, 2, \ldots, 6$ and $m, k = 1, 2, 3$ refer to different directions within the material coordinate system, as shown in Figure 2.5. The above equations can be re-written in the following form, which is often used for applications that involve sensing:

$$\varepsilon_i = S_{ij}^D \sigma_j + g_{mi} D_m \tag{2.3}$$

$$E_i = g_{mi} \sigma_i + \beta_{ik}^\sigma D_k \tag{2.4}$$

where

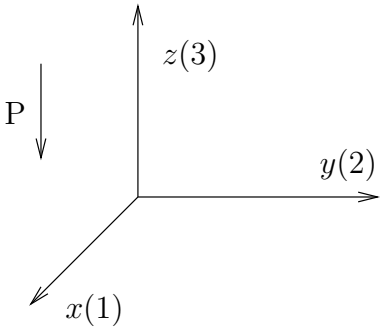

#	Axis
1	x
2	y
3	z
4	Shear around x
5	Shear around y
6	Shear around z

Figure 2.5. Axis nomenclature

σ ... stress vector (N/m^2)
ε ... strain vector (m/m)
E... vector of applied electric field (V/m)
ξ ... permitivity (F/m)
d ... matrix of piezoelectric strain constants (m/V)
S ... matrix of compliance coefficients (m^2/N)
D... vector of electric displacement (C/m^2)
g ... matrix of piezoelectric constants (m^2/C)
β ... impermitivity component (m/F)

Furthermore, the superscripts D, E, and σ represent measurements taken at constant electric displacement, constant electric field and constant stress.

Equations (2.1) and (2.3) express the converse piezoelectric effect, which describe the situation when the device is being used as an actuator. Equations (2.2) and (2.4), on the other hand, express the direct piezoelectric effect, which deals with the case when the transducer is being used as a sensor. The converse effect is often used to determine the piezoelectric coefficients.

In matrix form, Equations (2.1)-(2.4) can be written as:

$$\begin{bmatrix} \varepsilon_1 \\ \varepsilon_2 \\ \varepsilon_3 \\ \varepsilon_4 \\ \varepsilon_5 \\ \varepsilon_6 \end{bmatrix} = \begin{bmatrix} S_{11} & S_{12} & S_{13} & S_{14} & S_{15} & S_{16} \\ S_{21} & S_{22} & S_{23} & S_{24} & S_{25} & S_{26} \\ S_{31} & S_{32} & S_{33} & S_{34} & S_{35} & S_{36} \\ S_{41} & S_{42} & S_{43} & S_{44} & S_{45} & S_{46} \\ S_{51} & S_{52} & S_{53} & S_{54} & S_{55} & S_{56} \\ S_{61} & S_{62} & S_{63} & S_{64} & S_{65} & S_{66} \end{bmatrix} \begin{bmatrix} \sigma_1 \\ \sigma_2 \\ \sigma_3 \\ \tau_{23} \\ \tau_{31} \\ \tau_{12} \end{bmatrix} + \begin{bmatrix} d_{11} & d_{21} & d_{31} \\ d_{12} & d_{22} & d_{32} \\ d_{13} & d_{23} & d_{33} \\ d_{14} & d_{24} & d_{34} \\ d_{15} & d_{25} & d_{35} \\ d_{16} & d_{26} & d_{36} \end{bmatrix} \begin{bmatrix} E_1 \\ E_2 \\ E_3 \end{bmatrix} \tag{2.5}$$

and

$$\begin{bmatrix} D_1 \\ D_2 \\ D_3 \end{bmatrix} = \begin{bmatrix} d_{11} & d_{12} & d_{13} & d_{14} & d_{15} & d_{16} \\ d_{21} & d_{22} & d_{23} & d_{24} & d_{25} & d_{26} \\ d_{31} & d_{32} & d_{33} & d_{34} & d_{35} & d_{36} \end{bmatrix} \begin{bmatrix} \sigma_1 \\ \sigma_2 \\ \sigma_3 \\ \sigma_4 \\ \sigma_5 \\ \sigma_6 \end{bmatrix} + \begin{bmatrix} e_{11}^{\sigma} & e_{12}^{\sigma} & e_{13}^{\sigma} \\ e_{21}^{\sigma} & e_{22}^{\sigma} & e_{23}^{\sigma} \\ e_{31}^{\sigma} & e_{32}^{\sigma} & e_{33}^{\sigma} \end{bmatrix} \begin{bmatrix} E_1 \\ E_2 \\ E_3 \end{bmatrix}. \tag{2.6}$$

Some texts use the following notation for shear strain

$$\gamma_{23} = \varepsilon_4$$
$$\gamma_{31} = \varepsilon_5$$
$$\gamma_{12} = \varepsilon_6$$

and for shear stress

$$\tau_{23} = \sigma_4$$
$$\tau_{31} = \sigma_5$$
$$\tau_{12} = \sigma_6.$$

Assuming that the device is poled along the axis 3, and viewing the piezoelectric material as a transversely isotropic material, which is true for piezoelectric ceramics, many of the parameters in the above matrices will be either zero, or can be expressed in terms of other parameters. In particular, the non-zero compliance coefficients are:

$$S_{11} = S_{22}$$
$$S_{13} = S_{31} = S_{23} = S_{32}$$
$$S_{12} = S_{21}$$
$$S_{44} = S_{55}$$
$$S_{66} = 2(S_{11} - S_{12}).$$

The non-zero piezoelectric strain constants are

$$d_{31} = d_{32}$$

and

$$d_{15} = d_{24}.$$

Finally, the non-zero dielectric coefficients are $e_{11}^{\sigma} = e_{22}^{\sigma}$ and e_{33}^{σ}. Subsequently, the equations (2.5) and (2.6) are simplified to:

$$\begin{bmatrix}\varepsilon_1\\ \varepsilon_2\\ \varepsilon_3\\ \varepsilon_4\\ \varepsilon_5\\ \varepsilon_6\end{bmatrix} = \begin{bmatrix}S_{11} & S_{12} & S_{13} & 0 & 0 & 0\\ S_{12} & S_{11} & S_{13} & 0 & 0 & 0\\ S_{13} & S_{13} & S_{33} & 0 & 0 & 0\\ 0 & 0 & 0 & S_{44} & 0 & 0\\ 0 & 0 & 0 & 0 & S_{44} & 0\\ 0 & 0 & 0 & 0 & 0 & 2(S_{11}-S_{12})\end{bmatrix}\begin{bmatrix}\sigma_1\\ \sigma_2\\ \sigma_3\\ \tau_{23}\\ \tau_{31}\\ \tau_{12}\end{bmatrix} + \begin{bmatrix}0 & 0 & d_{31}\\ 0 & 0 & d_{31}\\ 0 & 0 & d_{33}\\ 0 & d_{15} & 0\\ d_{15} & 0 & 0\\ 0 & 0 & 0\end{bmatrix}\begin{bmatrix}E_1\\ E_2\\ E_3\end{bmatrix} \tag{2.7}$$

and

$$\begin{bmatrix}D_1\\ D_2\\ D_3\end{bmatrix} = \begin{bmatrix}0 & 0 & 0 & 0 & d_{15} & 0\\ 0 & 0 & 0 & d_{15} & 0 & 0\\ d_{31} & d_{31} & d_{33} & 0 & 0 & 0\end{bmatrix}\begin{bmatrix}\sigma_1\\ \sigma_2\\ \sigma_3\\ \sigma_4\\ \sigma_5\\ \sigma_6\end{bmatrix} + \begin{bmatrix}e_{11}^{\sigma} & 0 & 0\\ 0 & e_{11}^{\sigma} & 0\\ 0 & 0 & e_{33}^{\sigma}\end{bmatrix}\begin{bmatrix}E_1\\ E_2\\ E_3\end{bmatrix}.$$

The "piezoelectric strain constant" d is defined as the ratio of developed free strain to the applied electric field. The subscript d_{ij} implies that the electric field is applied or charge is collected in the i direction for a displacement or force in the j direction. The physical meaning of these, as well as other piezoelectric constants, will be explained in the following section.

The actuation matrix in (2.5) applies to PZT materials. For actuators made of PVDF materials, this matrix should be modified to

$$\begin{bmatrix}0 & 0 & d_{31}\\ 0 & 0 & d_{32}\\ 0 & 0 & d_{33}\\ 0 & d_{25} & 0\\ d_{15} & 0 & 0\\ 0 & 0 & 0\end{bmatrix}.$$

This reflects the fact that in PVDF films the induced strain is nonisotropic on the surface of the film. Hence, an electric field applied in the direction of the polarization vector will result in different strains in 1 and 2 directions.

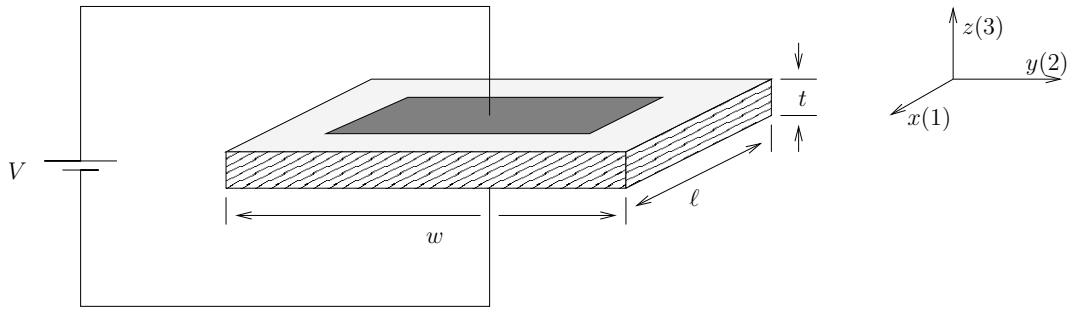

Figure 2.6. A piezoelectric transducer arrangement for d_{31} measurement

2.5 Piezoelectric Coefficients

This section reviews the physical meaning of some of the piezoelectric coefficients introduced in the previous section. Namely d_{ij}, g_{ij}, S_{ij} and e_{ij}.

2.5.1 Piezoelectric Constant d_{ij}

The piezoelectric coefficient d_{ij} is the ratio of the strain in the j-axis to the electric field applied along the i-axis, when all external stresses are held constant. In Figure 2.6, a voltage of V is applied to a piezoelectric transducer which is polarized in direction 3. This voltage generates the electric field

$$E_3 = \frac{V}{t}$$

which strains the transducer. In particular

$$\varepsilon_1 = \frac{\Delta\ell}{\ell}$$

in which

$$\Delta_\ell = \frac{d_{31} V \ell}{t}.$$

The piezoelectric constant d_{31} is usually a negative number. This is due to the fact that application of a positive electric field will generate a positive strain in direction 3.

Another interpretation of d_{ij} is the ratio of short circuit charge per unit area flowing between connected electrodes perpendicular to the j direction to the stress applied in the i direction. As shown in Figure 2.7, once a force F is applied to the transducer, in the 3 direction, it generates the stress

$$\sigma_3 = \frac{F}{\ell w}$$

which results in the electric charge

$$q = d_{33} F$$

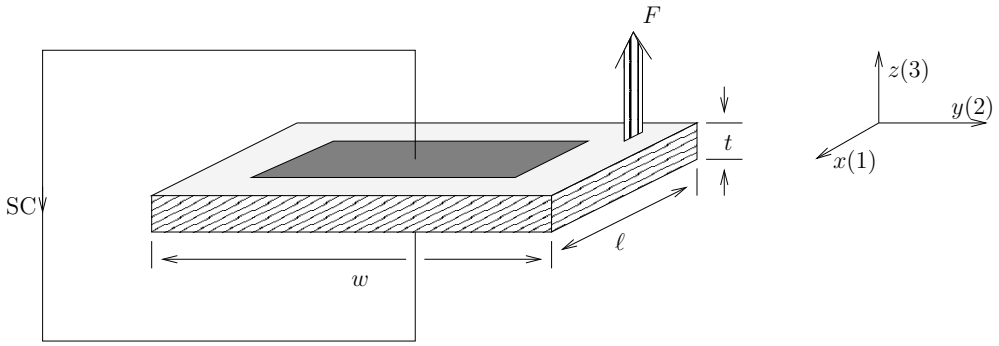

Figure 2.7. Charge deposition on a piezoelectric transducer - An equal, but opposite force, F, is not shown

flowing through the short circuit.

If a stress is applied equally in 1, 2 and 3 directions, and the electrodes are perpendicular to axis 3, the resulting short-circuit charge (per unit area), divided by the applied stressed is denoted by d_p.

2.5.2 Piezoelectric Constant g_{ij}

The piezoelectric constant g_{ij} signifies the electric field developed along the i-axis when the material is stressed along the j-axis. Therefore, in Figure 2.8 the applied force F, results in the voltage

$$V = \frac{g_{31}F}{w}.$$

Another interpretation of g_{ij} is the ratio of strain developed along the j-axis to the charge (per unit area) deposited on electrodes perpendicular to the i-axis. Therefore, in Figure 2.9, if an electric charge of Q is deposited on the surface electrodes, the thickness of the piezoelectric element will change by

$$\Delta\ell = \frac{g_{31}Q}{w}.$$

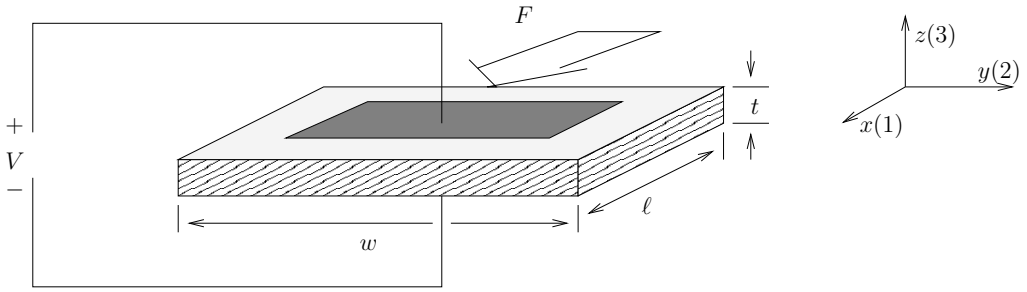

Figure 2.8. An open-circuited piezoelectric transducer under a force in direction 1 - An equal, but opposite force, F, is not shown

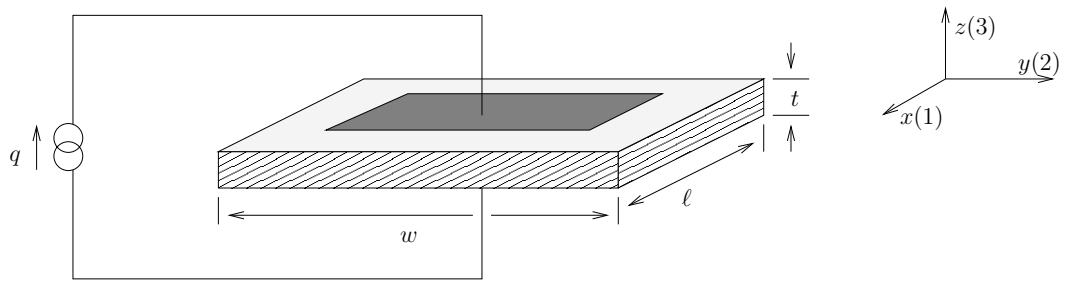

Figure 2.9. A piezoelectric transducer subject to applied charge

2.5.3 Elastic Compliance S_{ij}

The elastic compliance constant S_{ij} is the ratio of the strain the in i-direction to the stress in the j-direction, given that there is no change of stress along the other two directions. Direct strains and stresses are denoted by indices 1 to 3. Shear strains and stresses are denoted by indices 4 to 6. Subsequently, S_{12} signifies the direct strain in the 1-axis when the device is stressed along the 2-axis, and stresses along directions 1 and 3 are unchanged. Similarly, S_{44} refers to the shear strain around the 2-axis due to the shear stress around the same axis.

A superscript "E" is used to state that the elastic compliance S_{ij}^E is measured with the electrodes short-circuited. Similarly, the superscript "D" in S_{ij}^D denotes that the measurements were taken when the electrodes were left open-circuited. A mechanical stress results in an electrical response that can increase the resultant strain. Therefore, it is natural to expect S_{ij}^E to be smaller than S_{ij}^D. That is, a short-circuited piezo has a smaller Young's modulus of elasticity than when it is open-circuited.

2.5.4 Dielectric Coefficient, e_{ij}

The dielectric coefficient e_{ij} determines the charge per unit area in the i-axis due to an electric field applied in the j-axis. In most piezoelectric materials, a field applied along the j-axis causes electric displacement only in that direction. The relative dielectric constant, defined as the ratio of the absolute permitivity of the material by permitivity of free space, is denoted by K. The superscript σ in e_{11}^{σ} refers to the permitivity for a field applied in the 1 direction, when the material is not restrained.

2.5.5 Piezoelectric Coupling Coefficient k_{ij}

The piezoelectric coefficient k_{ij} represents the ability of a piezoceramic material to transform electrical energy to mechanical energy and *vice versa*. This transformation of energy between mechanical and electrical domains is employed in both sensors and actuators made from piezoelectric materials. The

ij index indicates that the stress, or strain is in the direction j, and the electrodes are perpendicular to the i-axis. For example, if a piezoceramic is mechanically strained in direction 1, as a result of electrical energy input in direction 3, while the device is under no external stress, then the ratio of stored mechanical energy to the applied electrical energy is denoted as k_{31}^2.

There are a number of ways that k_{ij} can be measured. One possibility is to apply a force to the piezoelectric element, while leaving its terminals open-circuited. The piezoelectric device will deflect, similar to a spring. This deflection Δ_z, can be measured and the mechanical work done by the applied force F can be determined

$$\mathcal{W}_M = \frac{F\Delta_z}{2}.$$

Due to the piezoelectric effect, electric charges will be accumulated on the transducer's electrodes. This amounts to the electrical energy

$$\mathcal{W}_E = \frac{Q^2}{2C_p}$$

which is stored in the piezoelectric capacitor. Therefore,

$$\begin{aligned} k_{33} &= \sqrt{\frac{\mathcal{W}_E}{\mathcal{W}_M}} \\ &= \frac{Q}{\sqrt{F\Delta_z C_p}}. \end{aligned}$$

The coupling coefficient can be written in terms of other piezoelectric constants. In particular

$$\begin{aligned} k_{ij}^2 &= \frac{d_{ij}^2}{S_{ij}^E e_{ij}^\sigma} \\ &= g_{ij} d_{ij} E_p, \end{aligned} \tag{2.8}$$

where E_p is the Young's modulus of elasticity of the piezoelectric material.

When a force is applied to a piezoelectric transducer, depending on whether the device is open-circuited or short-circuited, one should expect to observe different stiffnesses. In particular, if the electrodes are short-circuited, the device will appear to be "less stiff". This is due to the fact that upon the application of a force, the electric charges of opposite polarities accumulated on the electrodes cancel each other. Subsequently no electrical energy can be stored in the piezoelectric capacitor. Denoting short-circuit stiffness and open-circuit stiffness respectively as K_{sc} and K_{oc}, it can be proved that

$$\frac{K_{oc}}{K_{sc}} = \frac{1}{1-k^2}.$$

2.6 Piezoelectric Sensor

When a piezoelectric transducer is mechanically stressed, it generates a voltage. This phenomenon is governed by the direct piezoelectric effect (2.2). This property makes piezoelectric transducers suitable for sensing applications. Compared to strain gauges, piezoelectric sensors offer superior signal to noise ratio, and better high-frequency noise rejection. Piezoelectric sensors are, therefore, quite suitable for applications that involve measuring low strain levels. They are compact, easy to embed and require moderate signal conditioning circuitry.

If a PZT sensor is subject to a stress field, assuming the applied electric field is zero, the resulting electrical displacement vector is:

$$\begin{Bmatrix} D_1 \\ D_2 \\ D_3 \end{Bmatrix} = \begin{bmatrix} 0 & 0 & 0 & 0 & d_{15} & 0 \\ 0 & 0 & 0 & d_{15} & 0 & 0 \\ d_{31} & d_{31} & d_{33} & 0 & 0 & 0 \end{bmatrix} \begin{Bmatrix} \sigma_1 \\ \sigma_2 \\ \sigma_3 \\ \tau_{23} \\ \tau_{31} \\ \tau_{12} \end{Bmatrix}.$$

The generated charge can be determined from

$$q = \int\int \begin{bmatrix} D_1 & D_2 & D_3 \end{bmatrix} \begin{bmatrix} dA_1 \\ dA_2 \\ dA_3 \end{bmatrix},$$

where dA_1, dA_2 and dA_3 are, respectively, the differential electrode areas in the 2-3, 1-3 and 1-2 planes. The generated voltage V_p is related to the charge via

$$V_p = \frac{q}{C_p},$$

where C_p is capacitance of the piezoelectric sensor.

Having measured the voltage, V_p, strain can be determined by solving the above integral. If the sensor is a PZT patch with two faces coated with thin electrode layers, *e.g.* the patch in Figure 2.4, and if the stress field only exists along the 1-axis, the capacitance can be determined from

$$C_p = \frac{\ell w e_{33}^{\sigma}}{t}.$$

Assuming the resulting strain is along the 1-axis, the sensor voltage is found to be

$$V_s = \frac{d_{31} E_p w}{C_p} \int_{\ell} \varepsilon_1 dx, \tag{2.9}$$

where E_p is the Young's modulus of the sensor and ε_1 is averaged over the sensor's length. The strain can then be calculated from

$$\varepsilon_1 = \frac{C_p V_s}{d_{31} E_p \ell w}. \tag{2.10}$$

In deriving the above equation, the main assumption was that the sensor was strained only along 1-axis. If this assumption is violated, which is often the case, then (2.10) should be modified to

$$\varepsilon_1 = \frac{C_p V_s}{(1-\nu) d_{31} E_p \ell w},$$

where ν is the Poisson's ratio[4].

2.7 Piezoelectric Actuator

Consider a beam with a pair of collocated piezoelectric transducers bonded to it as shown in Figure 2.10. The purpose of actuators is to generate bending in the beam by applying a moment to it. This is done by applying equal voltages, of 180° phase difference, to the two patches. Therefore, when one patch expands, the other contracts. Due to the phase difference between the voltages applied to the two actuators, only pure bending of the beam will occur, without any excitation of longitudinal waves. The analysis presented in this section follows the research reported in references [42, 11, 76, 53].

When a voltage V is applied to one of the piezoelectric elements, in the direction of the polarization vector, the actuator strains in direction 1 (the x-axis). Furthermore, the amount of free strain is given by

$$\varepsilon_p = \frac{d_{31} V}{t_p}, \tag{2.11}$$

where t_p represents the thickness of the piezoelectric actuator.

Since the piezoelectric patch is bonded to the beam, its movements are constrained by the stiffness of the beam. In the foregoing analysis perfect bonding of the actuator to the beam is assumed. In other words, the shearing effect of the non-ideal bonding layer is ignored [33]. Assuming that the strain distribution is linear across the thickness of the beam[5], we may write

$$\varepsilon(z) = \alpha z. \tag{2.12}$$

The above equation represents the strain distribution throughout the beam, and the piezoelectric patches, if the composite structure were bent, say by an external load, into a downward curvature. Subsequently, the portion of the beam above the neutral axis and the top patch would be placed in

[4] Notice that if $d_{31} \neq d_{32}$, *e.g.* if the sensor is a PVDF film, then this expression for strain must be changed to $\varepsilon_1 = \frac{C_p V_s}{(1-\nu\frac{d_{32}}{d_{31}}) d_{31} E_p \ell w}$.

[5] This is consistent with the Kirchoff hypothesis of laminate plate theory[97].

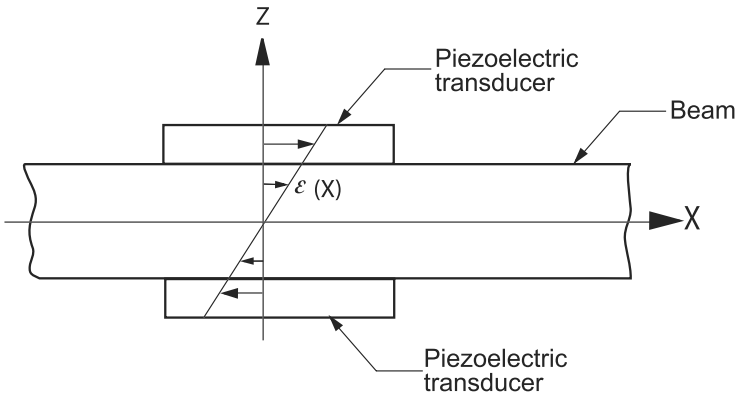

Figure 2.10. A beam with a pair of identical collocated piezoelectric actuators

tension, and the bottom half of the structure and the bottom patch in compression. Although, the strain is continuous on the beam-actuator surface, the stress distribution is discontinuous. In particular, using Hooke's law, the stress distribution within the beam is found to be

$$\sigma_b(z) = E_b \alpha z, \tag{2.13}$$

where E_b is the Young's modulus of elasticity of the beam. Since the two "identical" piezoelectric actuators are constrained by the beam, stress distributions inside the top and the bottom actuators can be written in terms of the total strain in each actuator (the strain that produces stress)

$$\sigma_p^t = E_p(\alpha z - \varepsilon_p) \tag{2.14}$$

$$\sigma_p^b = E_p(\alpha z + \varepsilon_p), \tag{2.15}$$

where E_p is the Young's modulus of elasticity of the piezoelectric material and the superscripts t and b refer to the top and bottom piezoelectric patches respectively. Applying moment equilibrium about the center of the beam[6] results in

$$\int_{-\frac{t_b}{2}-t_p}^{-\frac{t_b}{2}} \sigma_p^b(z) z dz + \int_{-\frac{t_b}{2}}^{\frac{t_b}{2}} \sigma_p(z) z dz + \int_{\frac{t_b}{2}}^{\frac{t_b}{2}+t_p} \sigma_p^t(z) z dz = 0. \tag{2.16}$$

After integration α is determined to be

$$\alpha = \frac{3E_p\left((\frac{t_b}{2}+t_p)^2 - (\frac{t_b}{2})^2\right)}{2\left(E_p\left\{(\frac{t_b}{2}+t_p)^3 - (\frac{t_b}{2})^3\right\} + E_b(\frac{t_b}{2})^3\right)}\varepsilon_p. \tag{2.17}$$

[6] Due to the symmetrical nature of the stress field, the integration need only be carried out starting from the centre of the beam, *i.e.* $\int_0^{\frac{t_b}{2}} \sigma_p(z) z dz + \int_{\frac{t_b}{2}}^{\frac{t_b}{2}+t_p} \sigma_p^t(z) z dz = 0$.

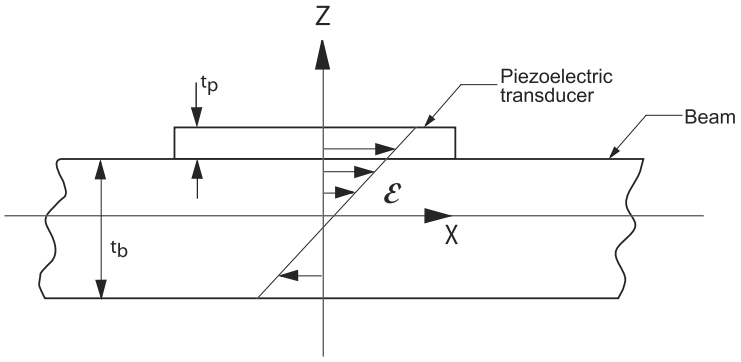

Figure 2.11. A beam with a single piezoelectric actuator

The induced moment intensity[7], M in the beam is then determined by integrating the triangular stress distribution across the beam:

$$M = E_b I \alpha, \tag{2.18}$$

where I is the beam's moment of inertia. Knowledge of M is crucial in determining the dynamics of the piezoelectric laminate beam.

If only one piezoelectric actuator is bonded to the beam, such as shown in Figure 2.11, then the strain distribution (2.12) needs to be modified to

$$\varepsilon(z) = (\alpha z + \varepsilon_0). \tag{2.19}$$

This expression for strain distribution across the beam thickness can be decomposed into two parts: the flexural component, αz and the longitudinal component, ε_0. Therefore, the beam extends and bends at the same time. This is demonstrated in Figure 2.12. The stress distribution inside the piezoelectric actuator is found to be

$$\sigma_p(z) = E_p(\alpha z + \varepsilon_0 - \varepsilon_p). \tag{2.20}$$

The two parameters, ε_0 and α can be determined by applying the moment equilibrium about the centre of the beam

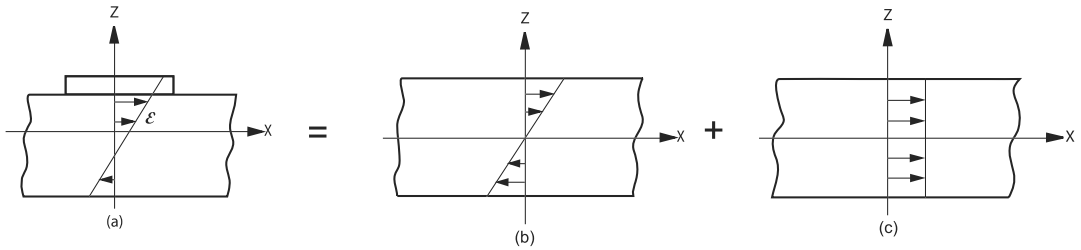

Figure 2.12. Decomposition of asymmetric stress distribution (a) into two parts: (b) flexural and (c) longitudinal components.

[7] moment per unit length

$$\int_{-\frac{t_b}{2}}^{\frac{t_b}{2}} \sigma_b(z) z dz + \int_{\frac{t_b}{2}}^{\frac{t_b}{2}+t_p} \sigma_p(z) z dz = 0 \tag{2.21}$$

and the force equilibrium along the x-axis

$$\int_{-\frac{t_b}{2}}^{\frac{t_b}{2}} \sigma_b(z) dz + \int_{\frac{t_b}{2}}^{\frac{t_b}{2}+t_p} \sigma_p(z) dz = 0. \tag{2.22}$$

Unlike the symmetric case, the force equilibrium condition (2.22) needs to be applied. This is due to the asymmetric distribution of strain throughout the beam. Solving (2.21) and (2.22) for ε_0 and α we obtain

$$\alpha = \frac{6E_b E_p t_b t_p (t_b + t_p)}{E_b^2 t_b^4 + E_p E_b (4t_b^3 t_p + 6t_b^2 t_p^2 + 4t_b t_p^3) + E_p^2 t_p} \varepsilon_p \tag{2.23}$$

and

$$\varepsilon_0 = \frac{\{E_b t_p^3 + E_p t_p^3\} E_p (t_b/2)}{E_b^2 t_b^4 + E_p E_b (4t_b^3 t_p + 6t_b^2 t_p^2 + 4t_b t_p^3) + E_p^2 t_p} \varepsilon_p. \tag{2.24}$$

The response of the beam to this form of actuation consists of a moment distribution

$$M_x = E_b I \alpha \tag{2.25}$$

and a longitudinal strain distribution

$$\varepsilon_x = \varepsilon_0. \tag{2.26}$$

It can be observed that the moment exerted on the beam by one actuator is not exactly half of that applied by two collocated piezoelectric actuators driven by 180° out-of-phase voltages. This arises from the fact that the Expressions (2.25) and (2.23) do not include the effect of the second piezoelectric actuator. However, if this effect is included by allowing for the stiffness of the second actuator in the derivations, while ensuring that the voltage applied to this patch is set to zero, then it can be shown that the resulting moment will be exactly half of that predicted by (2.18) and (2.17). The collocated situation is often used in vibration control applications, in which one piezoelectric transducer is used as an actuator while the other one is used as a sensor. This configuration is appealing for feedback control applications for reasons that will be explained in Chapter 3.

2.8 Piezoelectric 2D Actuation

This section is concerned with the use of piezoelectric actuators for excitation of two-dimensional structures, such as plates in pure bending. The analysis is similar to that presented in the previous section. A typical application is

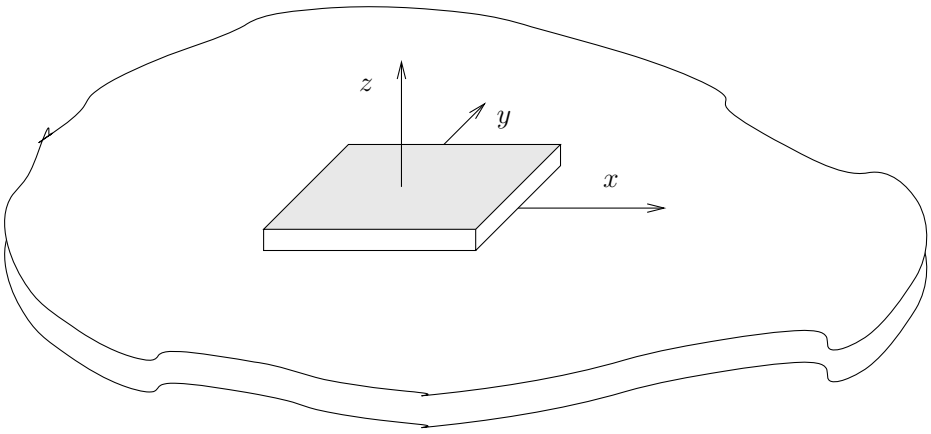

Figure 2.13. A piezoelectric actuator bonded to a plate

shown in Figure 2.13, which demonstrates a piezoelectric transducer bonded to the surface of a plate. It is also assumed that another identical transducer is bonded to the opposite side of the structure in a collocated fashion. If the two patches are driven by signals that are 180° out of phase, the resulting strain distribution, across the plate, will be linear as shown in Figure 2.14 a and b. That is,

$$\varepsilon_x = \alpha_x z \tag{2.27}$$

$$\varepsilon_y = \alpha_y z, \tag{2.28}$$

where α_x and α_y represent the strain distribution slopes in the $x-z$ and $y-z$ planes respectively.

Assuming that the piezoelectric material has similar properties in the 1 and 2 directions, *i.e.* $d_{31} = d_{32}$, the unconstrained strain associated with the actuator in both the x and y directions, under the voltage V, is given by

$$\varepsilon_p = \frac{d_{31} V}{t_p}.$$

Now the resulting stresses in the plate, in the x and y directions are

$$\sigma_x = \frac{E}{1-\nu^2}(\varepsilon_x + \nu\varepsilon_y)$$

and

$$\sigma_y = \frac{E}{1-\nu^2}(\varepsilon_y + \nu\varepsilon_x),$$

where ν is the Poisson's ratio of the plate material. Representing the stresses in the top piezoelectric patch as σ_x^p and σ_y^p, and the stresses in the bottom patch as $\tilde{\sigma}_x^p$ and $\tilde{\sigma}_y^p$, we may write

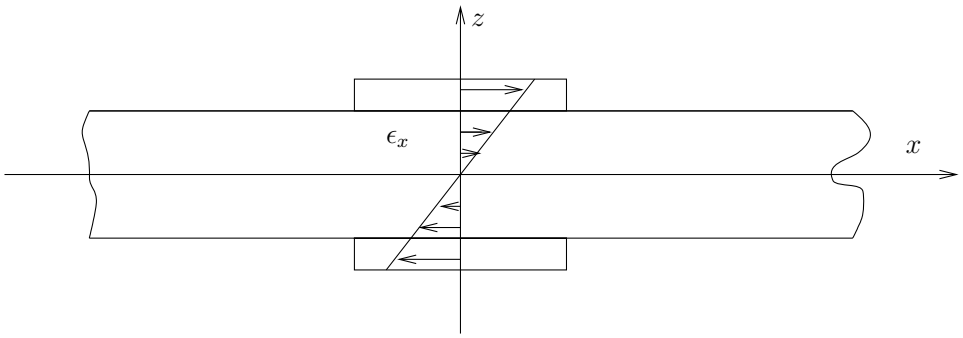

(a)

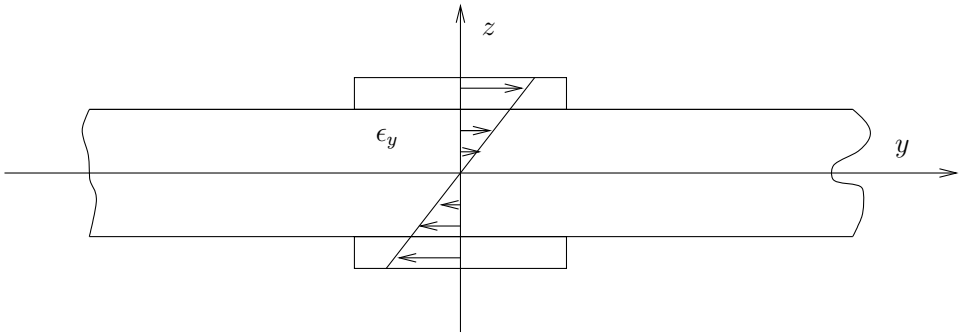

(b)

Figure 2.14. Two dimensional strain distribution in a plane with two collocated anti-symmetric piezoelectric actuators

$$\sigma_x^p = \frac{E_p}{1-\nu_p^2}\left\{\varepsilon_x + \nu_p\varepsilon_y - (1+\nu_p)\varepsilon_p\right\} \tag{2.29}$$

$$\tilde{\sigma}_x^p = \frac{E_p}{1-\nu_p^2}\left\{\varepsilon_x + \nu_p\varepsilon_y + (1+\nu_p)\varepsilon_p\right\} \tag{2.30}$$

$$\sigma_y^p = \frac{E_p}{1-\nu_p^2}\left\{\varepsilon_y + \nu_p\varepsilon_x - (1+\nu_p)\varepsilon_p\right\} \tag{2.31}$$

$$\tilde{\sigma}_y^p = \frac{E_p}{1-\nu_p^2}\left\{\varepsilon_y + \nu_p\varepsilon_x + (1+\nu_p)\varepsilon_p\right\}, \tag{2.32}$$

where ν_p is the Poisson's ratio of the piezoelectric material.

Given that ε_p is the same in both directions and that the plate is homogeneous, we may write

$$\varepsilon_x = \varepsilon_y = \varepsilon.$$

Subsequently, the strain distribution across the plate thickness can be written as

$$\varepsilon = \alpha_x z = \alpha_y z = \alpha z.$$

The condition of moment of equilibrium about the x and y axes can now be applied. That is,

$$\int_0^{\frac{t}{2}} \sigma_x z dz + \int_{\frac{t}{2}}^{\frac{t}{2}+t_p} \sigma_x^p z dz = 0$$

and

$$\int_0^{\frac{t}{2}} \sigma_y z dz + \int_{\frac{t}{2}}^{\frac{t}{2}+t_p} \sigma_y^p z dz = 0,$$

where t represents the plate's thickness. Integrating and solving for α gives

$$\alpha = \frac{3E_p\{(\frac{t_b}{2}+t_p)^2 - (\frac{t_b}{2})^2\}(1-\nu)}{2E_p\{(\frac{t_b}{2}+t_p)^3 - (\frac{t_b}{2})^3\}(1-\nu) + 2E(\frac{t_b}{2})^3(1-\nu_p)}\varepsilon_p.$$

The resulting moments in x and y directions are

$$M_x = M_y = EI\alpha. \tag{2.33}$$

For the symmetric case, *i.e.* when only one piezoelectric actuator is bonded to the plate, similar derivations to the previous section can be made.

2.9 Dynamics of a Piezoelectric Laminate Beam

In this section we explain how the dynamics of a beam with a number of collocated piezoelectric actuator/sensor pairs can be derived. At this stage we do not make any specific assumptions about the boundary conditions since we wish to keep the discussion as general as possible. However, we will explain how the effect of boundary conditions can be incorporated into the model.

Let us consider a setup as shown in Figure 2.15, where m identical collocated piezoelectric actuator/sensor pairs are bonded to a beam. The assumption that all piezoelectric transducers are identical is only adopted to simplify the derivations, and can be removed if necessary. The i^{th} actuator is exposed to a voltage of $v_{a_i}(t)$ and the voltage induced in the i^{th} sensor is $v_{p_i}(t)$.

We assume that the beam has a length of L, width of W, and thickness of t_b. Corresponding dimensions of each piezoelectric transducer are L_p, W_p, and t_p. Furthermore, we denote the transverse deflection of the beam at point x and time t by $z(x,t)$. The dynamics of such a structure are governed by the Bernoulli-Euler partial differential equation

$$E_b I \frac{\partial^4 z(x,t)}{\partial x^4} + \rho A_b \frac{\partial^2 z(x,t)}{\partial t^2} = \frac{\partial^2 M_x(x,t)}{\partial x^2}, \tag{2.34}$$

where ρ, A_b, E_b and I represent density, cross-sectional area, Young's modulus of elasticity and moment of inertia about the neutral axis of the beam respectively. The total moment acting on the beam is represented by $M_x(x,t)$, which is the sum of moments exerted on the beam by each actuator, *i.e.*

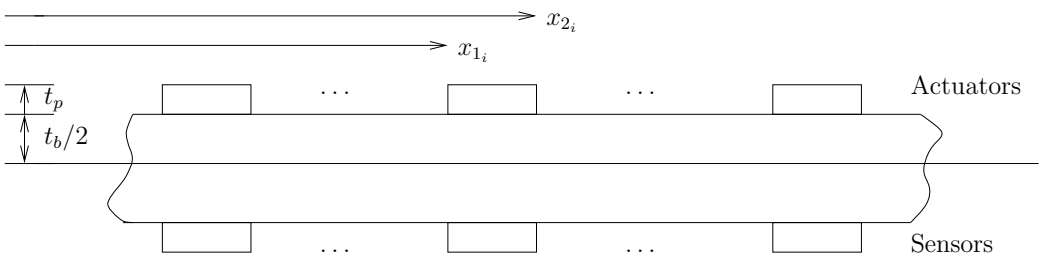

Figure 2.15. A beam with a number of collocated piezoelectric actuator/sensor pairs

$$M_x(x,t) = \sum_{i=1}^{m} M_{x_i}(x,t). \tag{2.35}$$

The moment exerted on the beam by the i^{th} actuator, $M_{x_i}(x,t)$ can be written as

$$M_{x_i}(x,t) = \bar{\kappa} v_{a_i}(t)\{u(x-x_{1_i}) - u(x-x_{2_i})\}, \tag{2.36}$$

where $u(x)$ represents the unit step function, *i.e.* $u(x) = 0$ for $x < 0$ and $u(x) = 1$ for $x \geq 0$. The term $\{u(x-x_{1_i}) - u(x-x_{2_i})\}$ is incorporated into (2.36) to account for the spatial placement of the i^{th} actuator. The constant $\bar{\kappa}$ can be determined from (2.11), (2.17) and (2.18). The forcing term in (2.34) can now be determined from Expressions (2.36) and (2.35), and using the following property of Dirac delta function

$$\int_{-\infty}^{\infty} \delta^{(n)}(t-\theta)\phi(t)dt = (-1)^n \phi^{(n)}(\theta), \tag{2.37}$$

where $\delta^{(n)}$ is the n^{th} derivative of δ, and ϕ is a continuous function of θ [111]. Having determined the expression for the forcing function in (2.34) we can now proceed to solving the partial differential equation. One approach to solving this PDE is based on using the modal analysis approach [130]. In this technique the solution of the PDE is assumed to be of the form

$$z(x,t) = \sum_{k=1}^{\infty} w_k(x) q_k(t). \tag{2.38}$$

Here $w_k(x)$, known as the modeshape, is the eigenfunction which is determined from the eigenvalue problem obtained by substituting (2.38) into (2.34) and using the following orthogonality properties [130]

$$\int_0^L w_k(x) w_p(x) dx = \delta_{kp} \tag{2.39}$$

$$\int_0^L \frac{E_b I}{\rho A_b} \frac{d^4 w_k(x)}{dx^4} w_p(x) dx = \omega_k^2 \delta_{kp}, \tag{2.40}$$

where ω_k describes the k^{th} natural frequency of the beam and δ_{kp} is the Kroneker delta function, *i.e.*

$$\delta_{kp} = \begin{cases} 1, & k = p \\ 0, & \text{otherwise} \end{cases}$$

A solution to the eigenvalue problem requires precise knowledge of boundary conditions. For specific boundary conditions, *e.g.* simply-supported and cantilevered, mode shapes and resonance frequencies can be determined analytically from the eigenvalue problem. For further details, the reader is referred to [130] and [50].

A set of uncoupled ordinary differential equations can be obtained from (2.34) using the orthogonality properties (2.39) and (2.40) and the property (2.37), as well as (2.38). It can be shown that the ordinary differential equations are of the form:

$$\ddot{q}_k(t) + \omega_k^2 q_k(t) = \frac{\bar{\kappa}}{\rho A_b} \sum_{i=1}^{m} \psi_{k_i} v_{a_i}(t), \tag{2.41}$$

where $k = 1, 2, \ldots$ and $q_k(t)$ is the generalized coordinate of the k^{th} mode. Furthermore, the parameter ψ_{k_i} is found to be:

$$\psi_{k_i} = \int_0^L w_k(x) \left\{ \delta'(x - x_{1_i}) - \delta'(x - x_{2_i}) \right\} dx \tag{2.42}$$

$$= w_k'(x_{2_i}) - w_k'(x_{1_i}), \tag{2.43}$$

where $f'(x)$ represents the first derivative of the function f with respect to x, and we have used (2.37) to obtain (2.43) from (2.42).

To this end we point out that the differential equation (2.41) does not contain a term to account for the natural damping associated with the beam. The presence of damping can be incorporated into (2.41) by adding the term $2\zeta_k \dot{q}_k(t)$ to (2.41). This results in the differential equation

$$\ddot{q}_k(t) + 2\zeta_k \omega_k \dot{q}_k(t) + \omega_k^2 q_k(t) = \frac{\bar{\kappa}}{\rho A_b} \sum_{i=1}^{m} \psi_{k_i} v_{a_i}(t). \tag{2.44}$$

Applying the Laplace transform to (2.44), assuming zero initial conditions, we obtain the following transfer function from the vector of applied actuator voltages $V_a(s) = [v_{a_1}(s), \ldots, v_{a_m}(s)]$ to the beam deflection $z(x, s)$ at location x

$$G(x, s) = \gamma \sum_{i=1}^{\infty} \frac{w_k(x) \bar{\psi}_k'}{s^2 + 2\zeta_k \omega_k s + \omega_k^2}, \tag{2.45}$$

where $\gamma = \frac{\bar{\kappa}}{\rho A_b}$ and

$$\bar{\psi}_k = \begin{bmatrix} \psi_{k_1} \\ \vdots \\ \psi_{k_m} \end{bmatrix}.$$

The piezoelectric voltage induced in the i^{th} sensor can be obtained using Expression (2.9). That is,

$$v_{p_i}(t) = \frac{d_{31} E_p W_p}{C_p} \int_0^L \varepsilon_{x_i} dx.$$

The expression for the mechanical strain in the i^{th} sensor patch can be obtained from

$$\varepsilon_{x_i} = -\left(\frac{t_b}{2} + t_p\right) \frac{\partial^2 z}{\partial x^2}.$$

Now v_{p_i} is found to be

$$v_{p_i}(t) = \frac{-d_{31} E_p W_p \left(\frac{t_b}{2} + t_p\right)}{C_p} \sum_{k=1}^{\infty} \psi_{k_i} q_k(t). \tag{2.46}$$

Therefore, the transfer function matrix relating the voltages applied to the piezoelectric actuators $V_a(s) = [v_{a_1}(s), \ldots, v_{a_m}(s)]$ to the voltages measured at the piezoelectric sensors $V_p(s) = [v_{p_1}(s), \ldots, v_{p_m}(s)]$ is found to be:

$$G_{vv}(s) = \bar{\gamma} \sum_{k=1}^{\infty} \frac{\bar{\psi}_k \bar{\psi}_k'}{s^2 + 2\zeta_k \omega_k s + \omega_k^2}, \tag{2.47}$$

where

$$\bar{\gamma} = \frac{-d_{31} E_p W_p \left(\frac{t_b}{2} + t_p\right) \bar{\kappa}}{C_p \rho A_b}.$$

To this end we need to explain how the systems represented by Infinite Series (2.47) and (2.45) can be approximated with finite dimensional models. In any controller design scenario we may only be interested in designing a controller for a finite bandwidth. If N modes of the structure lie within that bandwidth of interest, the series (2.47) and (2.45) are often truncated to obtain a finite dimensional model of the structure, which is of minimum dimensions. While the truncation may not be of concern in non-collocated models, *e.g.* (2.45), it can be a serious problem for a collocated system, *e.g.* (2.47). Truncation of a collocated model can result in perturbations in open-loop zeros of the system, which in the worst case can cause closed-loop instabilities, and in the best case will contribute to the loss of closed-loop performance [34].

A number of techniques have been proposed to compensate for the effect of truncated out-of-bandwidth modes on collocated structural models. The reader is referred to [34, 207, 138, 135, 84] and references therein for an overview of such techniques. We do, however, point out that the truncation

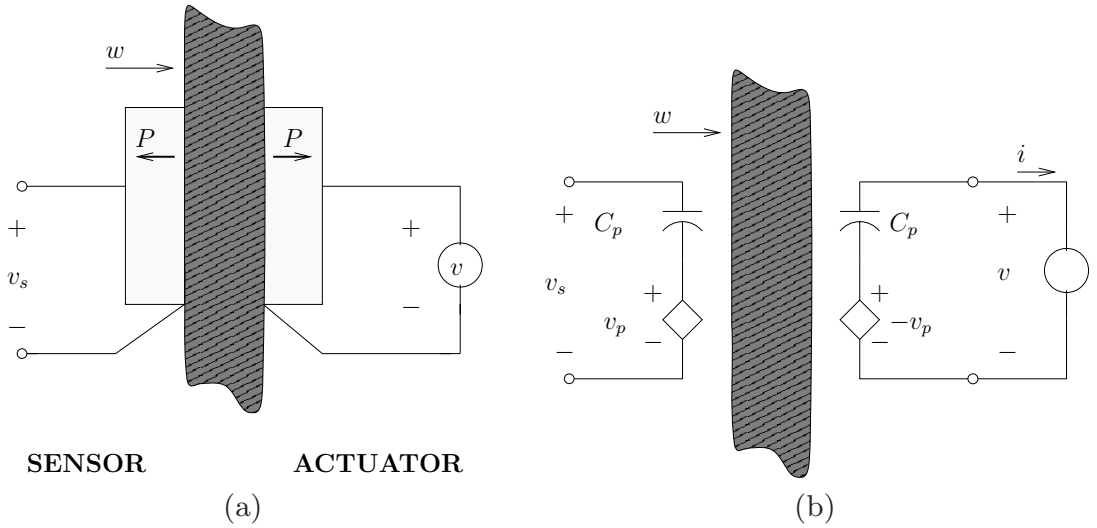

Figure 2.16. (a) A flexible structure with a pair of collocated piezoelectric transducers, and (b) its electrical equivalent model

error can be minimized by appending the truncated model by a feed-through term, *i.e.* to approximate (2.47) with

$$G_{vv}(s) = \bar{\gamma} \sum_{k=1}^{N} \frac{\bar{\psi}_k \bar{\psi}'_k}{s^2 + 2\zeta_k \omega_k s + \omega_k^2} + D.$$

If chosen properly, the addition of this feed-through term to the truncated model can result in an acceptable approximation. In this book, in most cases, we will use system identification to directly identify this parameter, as well as the rest of the dynamics of the system.

We conclude this chapter with an important observation that will be utilized in the forthcoming chapters. Figure 2.16 (a) illustrates a flexible structure with a collocated piezoelectric actuator/sensor pair. The piezoelectric transducer on the right functions as an actuator, and the one on the left as a sensor. What is of importance here is the electrical model of the system depicted in Figure 2.16 (b). Each piezoelectric transducer is modeled as a capacitor in series with a strain-dependent voltage source. The transfer function from the voltage applied to the actuator, v to the voltage induced in the sensor, $v_s = v_p$ is given by (2.47). This observation is particularly important in designing piezoelectric shunts, and to identify the connection between piezoelectric shunt damping and feedback control of a collocated system. This will be discussed in more detail in Chapter 5.

2.10 Active and Macro Fiber Composite Transducers

Active Fiber Composites (AFCs) are an alternative to traditional monolithic piezoelectric transducers. First proposed in 1992 [20], longitudinally polarized

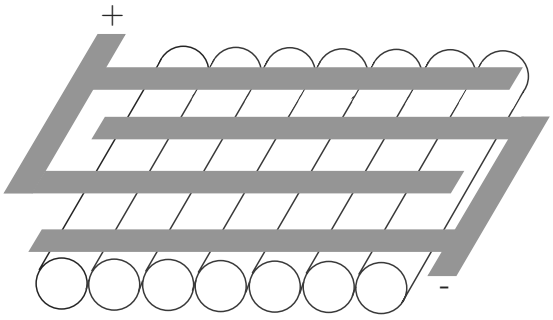

Figure 2.17. A piezoelectric Active Fiber Composite (AFC) comprised of piezoelectric fibers with interdigitated electrodes top and bottom

piezoelectric fibers, as shown in Figure 2.17, are encased in an epoxy resin with interdigitated electrodes laminated onto the top and bottom surfaces of the transducer. With an applied voltage, the interdigitated electrodes induce longitudinal electric fields along the length of each fiber. The original motivation was to increase the electromechanical coupling by utilizing the high d_{33} piezoelectric strain constant rather than the lesser d_{31} constant.

Active fiber composites have a number of practical advantages over traditional monolithic transducers [19]:

- The fibers are encapsulated by the printed polymer electrodes and epoxy resin thus increasing the reliability and service-life in harsh environments.
- The short length and diameter or the fibers together with their alignment along the length of the transducer increases the conformability of AFC transducers. They can be laminated onto structures with complex geometries and curvatures.
- AFC transducers are more robust to mechanical failure than monolithic transducers. In addition to their conformability, they can also tolerate local and incremental damage. If some of the fibers are fractured, the transducer will not be substantially damaged, in contrast, monolithic actuators will fracture and fail if they are stressed beyond their yield limit.
- AFCs have been reported to develop greater strains than monolithic actuators [19]. The strain actuation is also unidirectional.

Macro Fiber Composites (MFCs) [174] are similar in nature to AFCs as they utilize the direct d_{33} piezoelectric effect through the use of interdigitated electrodes. Rather than individual fibers, a monolithic transducer is simply cut into a number of long strips. The resulting transducer is conformable in one dimension and more robust to mechanical failure than monolithic patches.

The greatest disadvantages of AFC and MFC transducers is their high present cost, and the large voltages required to achieve the same actuation strain as monolithic transducers. The equivalent piezoelectric capacitance is also much lesser making them unsuitable as low-frequency strain sensors (see Section 6.2).

The low capacitance of AFC and MFC transducers also causes difficulties in the implementation of piezoelectric shunt damping systems, to be discussed in Chapter 4. Device capacitances of less than 50 nF have been deemed impractical for shunt damping [18]. A performance comparison of monolithic, AFC, and MFC transducers in a passive shunt damping application can be found in references [18] and [148].

Although the piezoelectric transducers used throughout this book are exclusively monolithic, all of the techniques discussed in the proceeding chapters are equally as applicable to AFC and MFC variants. Indeed, from the control engineers viewpoint, transducer physics is usually lumped into a simplified electrical model, or identified as part of the structural system.